Oceanologia, 66 (4)/2024, 66404

https://doi.org/10.5697/YEIT8094

Dynamics of phytoplankton functional communities in the South China Sea in response to multiple simultaneous stressors and ENSO-related climate anomalies

Anthony Banyouko Ndah [1,2,3,*], Julien Di Pane [2]

Abstract
Phytoplankton is crucial in maintaining the functional integrity of marine ecosystems, shaping the delicate balance between the food web base and higher trophic levels. However, these organisms are also susceptible to environmental changes, with fundamental ecological implications. We investigated the response of four phytoplankton communities (diatoms, coccolithophores, chlorophytes, and cyanobacteria) to hydroclimatic parameters in the South China Sea (SCS) between 1998 and 2012, and ascertained the effects of El Niño and La Niña climatic anomalies on the niche preferences of these communities at interannual timescales. Overall, changes in temperature and NO_3 jointly explained 51% of phytoplankton variability. Cyanobacteria was the most generalist taxon, displaying tolerance to both El Niño and La Niña conditions, justifying its relatively high abundance, increasing trend, and spatial expansion. Coccolithophore, the second most abundant community mainly in northern SCS was associated with La Niña-related conditions while diatoms were primarily associated with El Niño but displayed tolerance to both climatic regimes and a strong positive response to iron. Finally, chlorophytes were marginal under both El Niño and La Niña conditions indicating that inherent hydrographic constraints and competition limit their niche breadth and abundance. We concluded that non-linear interactions linked to El Niño drive interannual microbial dynamics in the SCS by modifying hydrographic and geochemical characteristics. Hence, we surmised that under accelerated ocean warming, cyanobacteria, and most likely dinoflagellates will dominate phytoplankton community structure with significant impacts on the food web and regional marine biogeochemistry.

Keywords
Phytoplankton; Environmental stressors; South China Sea; Multivariate statistics; Climate change

[1] *Plymouth Marine Laboratory, Plymouth, UK*
[2] *Alfred-Wegener-Institut, Helmholtz-Zentrum für Polar- und Meeresforschung, Biologische Anstalt Helgoland, Helgoland, Germany*
[3] *Universiti Brunei Darussalam, Jalan Tunku Link Gadong, Brunei Darussalam*
***Correspondence**: andah@pml.ac.uk (A.B. Ndah)

Received: 8 February 2021; **revised**: 5 September 2024; **accepted**: 6 September 2024

1. Introduction

The South China Sea (SCS, Figure 1) is a semi-enclosed marginal sea in the West-Pacific Ocean, situated in the tropical monsoon region between Lat. 4°–23°N and Lon. 105°–12°E. It covers an area of about 3.5×10^6 km^2 (IHO, 1953; Devantier and Turak, 2009), forming part of a network of six marginal seas collectively known as the 'Seas of East Asia' (Chen et al., 2006; IHO, 1953), inter-connected by natural processes, ocean currents, and shared living marine resources (Devantier and Turak, 2009). The sea is characterized by a mixture of water masses strongly influenced by runoff from over 100 major rivers (e.g. Mekong, Red, Xi Rivers) that drain the Asian mainland, major islands, and several important geologic/economically significant deltas, bays, and estuaries (Cheah et al., 2013; Wang et al., 2013; Huang and You, 2007; Wang and Ho, 2002; Milliman and Mie-e, 1995). The characteristics of the SCS amplified by recent changes in ocean-climatic conditions influence phytoplankton growth and primary production.

It is imperative to understand the nature and extent of the response of phytoplankton communities to changes in environmental conditions for several reasons. Firstly, phytoplankton constitutes the base of the marine food web responsible for approximately half of Earth's primary production (Field et al., 1998; Katz et al., 2004; Siswanto et

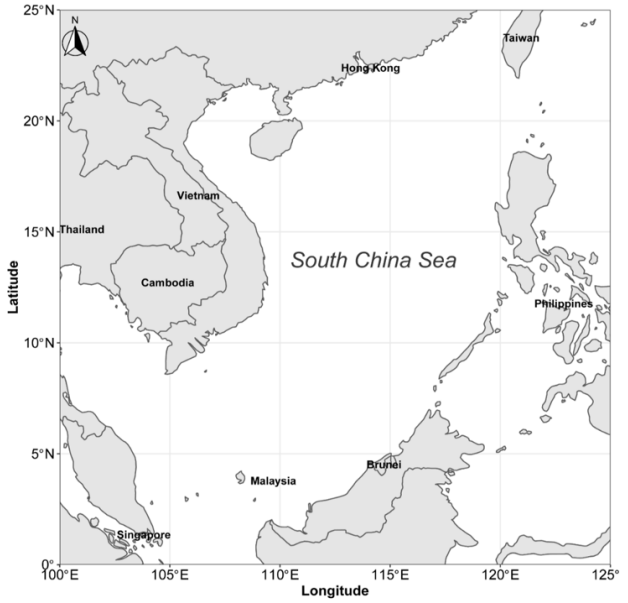

Figure 1. Map of the South China Sea (produced with the *naturalearth* package in R).

al., 2017). These microbial communities support fisheries production, a major source of livelihood and food security in the states surrounding the SCS, as well as drive marine biogeochemical cycling (Bjornstad and Dachevski, 2005) and carbon dioxide sequestration through the biological pump (Siswanto et al., 2017). The diverse spatiotemporal forcings of marine biogeochemistry (Chen et al., 2006) influencing primary production in the SCS are strongly modulated by the Southeast Asian Monsoons (N.E. monsoon – October/April and S.W. monsoon – May/September) at annual and intra-annual timescales. Latitudinal differences account for most of the spatial differences between the Northern and Southern South China Sea (e.g. Ndah et al., 2019). Temperature (SST or temp) is high throughout the year in the Southern South China Sea (SSCS), and in summer across northern SCS (NSCS) resulting in a strong vertical stratification of the water column (Tan et al., 2020). This induces surface oligotrophic characteristics and low surface nutrient concentrations (Wong et al., 2007). In the inter-tropical NSCS characterized by marked seasonal differences and a relatively large annual range of SST, enhanced stratification is a major feature in summer, while deep mixing dominates in winter. The simultaneous effects of SST and freshwater-induced stratification, and the dominance of anticyclonic gyres across the sea limit summer nutrient availability and primary production (Ning et al., 2004). In winter (N.E. monsoon), the persistent influence of monsoonal winds induces large-scale cyclonic circulation and eddy activity across the SCS, deepening the mixed layer, and enhancing autumn/winter production (Tan et al. 2020). Rivers are also among the main drivers of coastal biogeochemistry in the SCS. Vast agricultural lands around the SCS, especially in the North, drained by over 100 major rivers discharge tons of freshwater into the sea annually, inducing changes in sediment and nutrient loads, turbidity, and irradiance (IHO, 1953; Devantier and Turak, 2009; Turak and Devantier, 2011; Cheah et al., 2013; Wang et al., 2013). Atmospheric transport of trace elements is an important pathway of nutrients, contributing Fe, P, and other trace metals into the open oceanic regimes of the SCS (Zhang et al., 2007; Mackey et al., 2017). The deposition of Southeast Asian dust and other airborne particulate pollutants into the SCS deriving from biomass burning, pyrogenic soils (Hsu et al., 2014), and other pollution sources from manufacturing and automobiles (Zhang et al., 2007; Hsu et al., 2014) are important contributors of phosphates (P) and iron (Fe) in the SCS (Hsu et al., 2014). These abiotic mechanisms combined with alterations in SST and salinity profiles (Peng and Wang, 1999) drive phytoplankton dynamics and primary production through their interactions with nutrients (Peng and Wang, 1999; Hodgkiss and Lu, 2004; Palacz et al., 2011; Liao et al., 2012; Wang et al., 2014).

However, studies focusing on single-stressor effects, the response of single species, and the low temporal resolution characterizing much of the extant research are generally limited in their ability to effectively identify the dynamic ways by which global change processes affect phytoplankton communities (Moreno et al., 2022). Studies highlighting phytoplankton responses to changes in abiotic conditions in the SCS generally fall short due to their excessive focus on the monsoon-dominated intra-seasonal (e.g., Ning et al., 2004; Chen et al., 2006; Lin et al., 2010; Cheah et al., 2013; Li et al., 2015b; Cui et al., 2016) and seasonal (e.g. Wong et al., 2007; Shen et al., 2011; Dong et al., 2015; Li et al., 2015b) time scales. Moreover, most studies focus on primary production in NSCS (e.g. Liu et al., 2011; Cheah et al., 2013; Wang et al., 2013; Wei et al., 2018) in nearshore coastal locations (e.g. Wong et al., 2007; Qiu et al., 2010; Shen et al., 2011; Tian et al., 2014; Li et al., 2015a,b), often ignoring the reality that different plankton communities respond differently to sets of stressors. Furthermore, a mesocosm experiment, Moreno et al. (2022) established that the intensity of environmental change largely determines the effect size of pressures on phytoplankton communities, including the extent of shifts in functional traits and processes. Hence, an effective way to evaluate the intensity and effects of stressors is to track such pressures over extended periods and map out their simultaneous impacts on multiple communities. The present research therefore builds on a previous study by Ndah et al. (2019) describing patterns of phytoplankton dynamics at seasonal and interannual timescales across the SCS basin. The observed changes coincided with other reports of the increasing frequency and magnitude of harmful algal blooms and eutrophication in the SCS (Lu and Hodgkiss, 1999; Tang et al., 1999, 2004; Huppert et al., 2002; Chen et al., 2006;

Wang et al., 2010). El Niño Southern Oscillation (ENSO) has been identified as a major driver of inter-annual primary production in the SCS. El Niño modifies the physical oceanographic processes and influences nutrient availability (Palacz et al., 2011; Liao et al., 2012; Siswanto et al., 2017). However, the mechanistic processes by which the complex abiotic processes, including El Niño, influence the microbial ecology across the entire SCS basin remain poorly understood. Our study therefore seeks to identify and describe the main drivers of phytoplankton functional groups in the SCS at a basin-wide scale and link these to the effects of ENSO events on a mechanistic level.

2. Material and methods

2.1 Data sources

Assimilated monthly datasets of nutrients including monthly nitrate – NO_3 and iron – Fe and photosynthetically available radiation (PAR) were obtained from the NASA GIOVANNI portal. Time series of Phytoplankton functional groups (coccolithophores, cyanobacteria, diatoms, chlorophytes) and surface Chl-*a* measurements were also obtained from the GIOVANNI portal. The biological data were originally MODIS Aqua satellite measurements modeled with the NASA Ocean Biogeochemical Model to obtain monthly assimilated phytoplankton datasets (http://disc.sci.gsfc.nasa.gov/Giovanni/overview/index.html). The data covered the decade 1998–2012 with a spatial resolution of $0.667 \times 1.25°$ covering the South China Sea. This allowed for the effects of climatic anomalies to be easily detected and analyzed. Other environmental datasets were obtained from multiple databases archived by the Asia-Pacific Data Research Centre – APDRC (http://apdrc.soest.hawaii.edu). The variables included the Hadley Centre Sea surface temperature (HADSST1). Time-series of sea surface salinity (sal), wind speed, Mixed Layer Depth (MLD), and mass flux of river (runoff + calving) entering the ocean (river flux) were from the NOAA Geophysical Fluid Dynamics Lab ensemble coupled data assimilation. Rainfall data are based on the Tropical Rainfall Measuring Mission (TRMM) (Table 1). The Niño 4 index time-series dataset was obtained from Trenberth, Kevin and National Center for Atmospheric Research. The period 1998–2012 is ideal for studying the long-term variability of phytoplankton communities because of the lack of a warming trend in the South China Sea, implying the absence of a significant global warming signal. There is ample evidence that most parts of the tropical ocean cooled slightly after the super El Niño of 1997/98, including the SCS (Ndah, 2017). The statistical characteristics of the pre-transformed datasets are presented in Table 2.

2.2 Data analyses

Due to the different units of measurement and variable means, the data were transformed before running multivariate analyses. Data analyses were performed with the R software (R Development Core Team, 2008).

2.2.1 Redundancy analysis

Redundancy analysis RDA is a multivariate regression method showing the variation in a set of response variables (phytoplankton functional groups) using a set of explanatory variables (i.e., environmental parameters). RDA based on the method proposed by Borcard et al. (2011) was used to relate phytoplankton functional group structure to environmental variables implemented on tables of monthly phytoplankton abundances and environmental variables using the *vegan* package, with a threshold of significance set at an alpha of 0.05. The explanatory matrix comprised nine abiotic variables, including SST, PAR, MLD, sal, Fe and NO_3, wsp, river flux, and the Niño index. The response matrix was composed of phytoplankton functional groups including coccolithophores (calcareous nanoplankton), diatoms (siliceous phytoplankton), chlorophytes, and cyanobacteria. A permutation test (999 permutations) was performed to calculate the significance of the response. The collinearity of the variables was explored by a VIF (variable inflation factor). Variables with a VIF value > 10 indicating strong collinearities were eliminated and the model was reduced to a more parsimonious form. Variable selection was done by creating a null model (i.e. origin only) and then simultaneously performing a forward selection based on the null model and a backward selection based on the full model. This selection method performs a Monte Carlo permutation test (999 permutations) on each variable and stops once the model no longer improves with the addition or deletion of variables, based on the adjusted R^2 criterion (Blanchet et al., 2008). The simplified model was then permuted 999 times, along with the remaining variables. The simplified RDA was plotted with objects (samples) that are weighted sums of the response variables (taxa). This graphical method recommended by Borcard et al. (2011) is more robust to noise from environmental variables. In this representation, the distance between the response or explanatory variables is meaningless, as is the length of the arrows, and the degree of correlation is measured by the angle of the arrows. Once the environmental variables explaining the most changes in phytoplankton structure were highlighted, a selection of the four most important variables was done by partial RDA (RDAp), allowing us to obtain the amount of variation caused by each selected variable.

2.2.2 Variation partitioning analysis

A variation partitioning analysis – VPA (Mood, 1971; Peres-Neto et al. 2006), as proposed by Legendre and Legendre (2012), was performed on the fauna matrix and the four most important environmental variables previously identified. Variation partitioning provided the amount of variation explained by each of the four variables individually and the shared variation amongst them.

Table 1. List of variables and available datasets.

Category	Variable	Unit	Resolution	Timeframe	Source	ROI
Biological	Phytoplankton groups (coccolithophores, cyanobacteria, chlorophytes, diatoms), primary production (Chl-*a*)	$mg^{-1}\ m^{-3}$	Monthly, $0.67 \times 1.25°$	1998–2012	NASA Ocean Biogeochemical Model http://disc.sci.gsfc.nasa.gov/Giovanni/overview/index.html	Lat. 4°–23°N, Lon. 105°–12°E
Chemical	Nitrate (NO_3) Iron (Fe)	$\mu M\ l^{-1}$ $nM\ l^{-1}$	Monthly, $0.67 \times 1.25°$	1998–2012	NASA Ocean Biogeochemical Model http://disc.sci.gsfc.nasa.gov/Giovanni/overview/index.html	
Physical	Photosynthetically available radiation (par)	Einstein $m^{-2}\ day^{-1}$	Monthly, $0.67 \times 1.25°$	1998–2012	NASA Ocean Biogeochemical Model http://disc.sci.gsfc.nasa.gov/Giovanni/overview/index.html	
Physical	Temperature (SST)	°C	Monthly, $0.67 \times 1.25°$	1998–2012	ADSST, Asia-Pacific Data Research Centre – APDRC LAS 8.6 (http://apdrc.soest.hawaii.edu)	
Physical	Salinity (sal)	PSU $0.67 \times 1.25°$	Monthly,	1998–2012	NOAA GFDL ensemble coupled data assimilation, APDRC LAS 8.6 (http://apdrc.soest.hawaii.edu)	
Physical	Wind speed (wsp)	$m\ s^{-1}$	Monthly, $0.67 \times 1.25°$	1998–2012	NOAA GFDL ensemble coupled data assimilation, APDRC LAS 8.6 (http://apdrc.soest.hawaii.edu)	
Physical	Mixed Layer Depth (MLD)	m	Monthly, $0.67 \times 1.25°$	1998–2012	NOAA GFDL ensemble coupled data assimilation, APDRC LAS 8.6 (http://apdrc.soest.hawaii.edu)	
Physical	Niño index	unitless	Monthly	1998–2012	UCAR, https://climatedataguide.ucar.edu/climate-data/Ni~{n}o-sst-indices-Ni~{n}o-12-3-34-4-oni-and-tni	
Physical	Mass flux of river (runoff + calving) entering the ocean (river flux)	$kg\ m^{-3}$	Monthly, $0.67 \times 1.25°$	1998–2012	NOAA GFDL ensemble coupled data assimilation, APDRC LAS 8.6 (http://apdrc.soest.hawaii.edu)	

Table 2. Statistical characteristics of all variables.

Variables	Min.	Median	Mean	Max
Chl-*a* (mg^{-1} m^{-3})	0.09	0.12	0.12	0.19
Cyanobacteria (mg^{-1} m^{-3})	0.04	0.06	0.064	0.09
Coccolithophores (mg^{-1} m^{-3})	0.02	0.05	0.055	0.12
Diatom ($mg\ m^{-3}$)	0.0003	0.0024	0.0039	0.0265
Chlorophytes ($mg\ m^{-3}$)	0	5E-08	2.29E-06	6.88E-05
Niño Index	−1.83	0.18	−0.002	1.43
Salinity (PSU)	0.03	0.03	0.03	0.03
SST (°C)	26.56	28.73	28.44	30.02
PAR (Einstein m^2 day^{-1})	26.48	43.99	42.87	50.82
Wind speed ($m\ s^{-1}$)	3.71	5.4	5.429	7.73
MLD (m)	20.29	24.71	27.74	46.58
Fe ($nM\ l^{-1}$)	0.38	0.53	0.525	0.65
NO_3 ($\mu M\ l^{-1}$)	0.03	0.09	0.118	0.51
River ($kg\ m^{-3}$)	0.01	0.05	0.05	0.08

2.2.3 Within outlying mean indexes (WitOMI)

Phytoplankton inhabits various habitat types that are characteristic of a set of environmental conditions, considered niches of specific groups of species (Shih et al., 2020). For this reason, we used the WitOMI (sub-niche package in R-studio; Karasiewicz et al., 2017), an extension of the outlying mean index (OMI) (function 'niche' in the ade4 package; Dolédec et al., 2000) was used to assess the monthly log-transformed abundances of the phytoplankton community associations with the environment under ENSO conditions. The analysis consisted firstly of running a PCA using the normalized (mean equal to zero and standard deviation equal to one) environmental matrix to determine the position of the sampling units (SUs) in the multivariate space, with the origin of the PCA axes corresponding to the center of gravity (G) of the sampling units (i.e., represents the average mean habitat of the sampling domain). The OMI analysis was then performed on the standardized PCA values of environmental variables phytoplankton data. Finally, we performed the within outlying mean index (WitOMI) to identify the main environmental variables defining the ecological niche of phytoplankton communities and determine the sub-niches of these communities under the constraining impact of El Niño and La Niña conditions. The WitOMI split the total environmental envelope into sub-envelopes (E_K) based on a priori-defined factor comprising El Niño and La Niña years, creating a categorical variable with two levels (sub-envelopes E_K) representing the range of environmental conditions observed during El Niño and La Niña regimes. This analysis provided parameters for the taxa in each subset calculated from the environment's origin (G) or the subsets' origin (G_K). The origin G represented the overall mean environmental conditions while G_K (*G_La Niña* and *G_El Niño*) is the average of the environmental conditions encountered in each subset E_K (*E_La Niña* and *E_El Niño*). In both cases, the parameters obtained are the marginality (WitOMIG and WitOMIG_K), the tolerance (Tol$G$ and TolG_K), and the residual tolerance (RTol). WitOMIG and Tol$G$ are respectively the marginality and tolerance from the origin G, while WitOMIG_K and TolG_K are the marginality and tolerance regarding the origin of the subset G_K. We tested the statistical significances of the calculated marginalities (WitOMIG and WitOMIG_K) using the function subnikrandtest in the 'sub-niche' package. The null hypothesis of the former was that "each species within a subset was uninfluenced by its overall average condition" (WitOMIG). The latter's null hypothesis was that "each community within a subset was uninfluenced by its subset average condition" (WitOMIG_K), based on 999 permutations of the Monte Carlo permutation test. The function subkrandtest in the package 'sub niche' also checked for differences in the environmental conditions in the two subsets with the null hypothesis that "G_K is not different from the overall habitat condition, G".

3. Results

3.1 Annual changes in phytoplankton functional group structure in relation to environmental drivers

RDA was performed to explore temporal phytoplankton community structure and the influence of environmental conditions on phytoplankton functional groups, by integrating all variables, before being simplified to eliminate collinear and/or non-significant variables. Seven out of ten variables initially defined sufficed to obtain an R^2 adj equal to the complete model (0.64). Among the variables selected, SST, PAR, sal, NO_3, Fe ($p < 0.001$), wind speed ($p = 0.003$) and river flux ($p = 0.017$) explained 64% of the variations observed in the response matrix.

The results show yearly variations in taxonomic composition along the two first axes of Figure 2. Axes 1 and 2 explained 59% of the variation (47% and 12% respectively). The first axis explains 47% of the variation mainly characterized by differences between years of high coc-

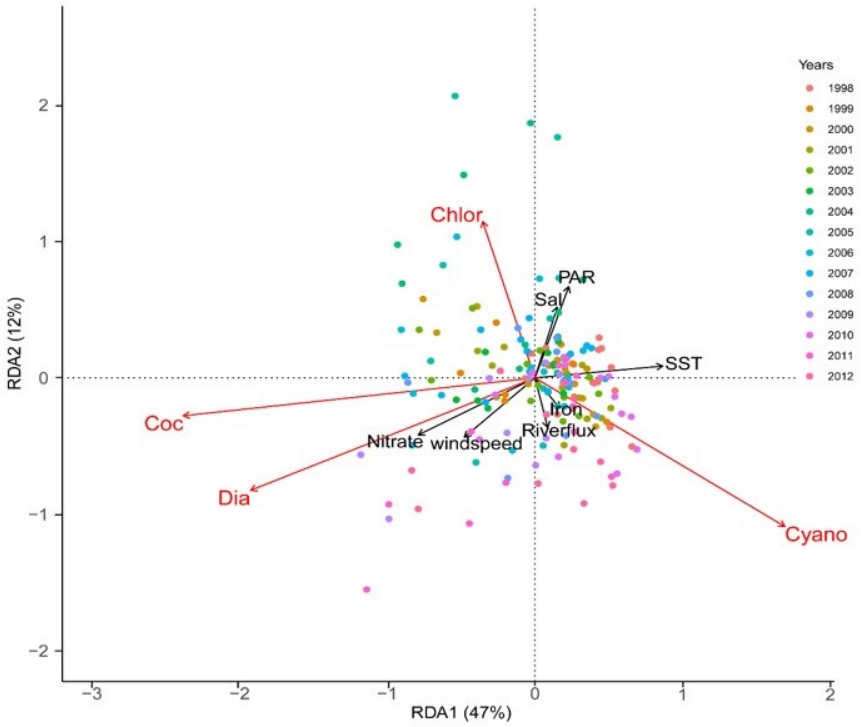

Figure 2. Parsimonious RDA (axes 1 and 2) with best variables selected by forward-selection. Each point corresponds to a sample (month). Coloured points represent years. Axes were created by annual abundances of diatoms (Dia), coccolithophores (Coc), cyanobacteria (Cya) and chlorophytes (Chlor).

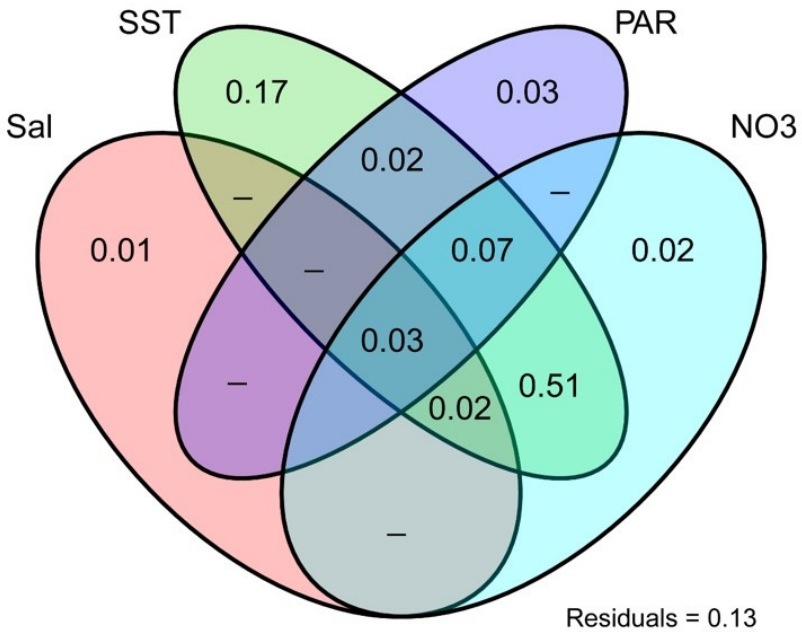

Figure 3. Variance partitioning analysis. Venn diagram showing the amount of variation explained in the phytoplankton assemblages by Sal, SST, PAR and NO_3 concentration. The greater the value of the contribution, the more the variable contributes to the variability of phytoplankton groups.

colithophores, diatoms, and cyanobacteria abundances, while the second axis (12% of variation explained) corresponded primarily to the abundance of chlorophytes at 999 permutations; $p < 0.05$. Coccolithophores and diatoms are affiliated strongly with the negative part of the RDA1 and cyanobacteria to the positive part of RDA1 (Figure 2).

Years of high diatom and coccolithophore concentrations occur in the positive part of the second axis (1998 –2004), while cyanobacteria affiliate to the positive part of RDA2, implying a negative correlation. Hence, the latter increased significantly between 2005 and 2012. SST had a positive influence on cyanobacteria but negatively affected diatoms and coccolithophores. In the period from 2005–2012, PAR and salinity appeared to have a positive effect on chlorophytes, with a low influence on the abundances of coccolithophores, diatoms, and cyanobacteria. River flux had a negative and positive influence on chlorophytes and cyanobacteria, respectively, while wsp and NO_3 had a positive influence on coccolithophores and diatoms. Annual differences in phytoplankton community structure were mainly driven by SST, NO_3, and sal, and PAR as the most parsimonious model selected only these variables (RDA; $F_{3,11} = 10.7, p < 0.001$).

The four most important variables (SST, sal, PAR, and NO_3) selected by RDAp were used to perform a variation partitioning by quantifying the variation explained by the most influential variables while controlling for the effect of the other variables (Figure 3).

Variation partitioning revealed that the individual explanatory variables were not orthogonal to one another. For this reason, two or more variables jointly explained some amount of variation, leading to a total variation of $< 77\%$, explained by four variables. SST, NO_3, PAR, and sal explained 82%, 65%, 15%, and 6% of the variation, respectively. In terms of pure effect, SST explained the bulk of the variability (17%) while PAR, NO_3, and sal accounted for 3%, 2%, and 1% of taxa variability. A large amount of variation was shared between SST and NO_3 (51%) and, to a lesser extent, among NO_3, PAR, and SST (7%). Together, all four variables shared only 3% of the total variation.

3.2 Phytoplankton niche differences under El Niño and La Niña regimes

WitOMI was used to model the influence of environmental parameters on phytoplankton communities associated with the El Niño and La Niña years. WitOMI analysis identified the influence of different environmental parameters on phytoplankton under El Niño and La Niña conditions. For all taxa, the marginality (OMI) was significant, implying the substantial influence of environmental variables (Monte Carlo permutation test, 999 permutations; $p < 0.01$) (Table 3). Of the total inertia explained by OMI (35%), the first two axes explained 99% of the projected inertia (97% and 2%, respectively) (Table 3). To compare the distribution of the phytoplankton functional groups between El Niño and La Niña, WitOMI defined subsets considering the environmental conditions encountered (Figure 4).

Table 3. Parameters and significance of the environmental envelope obtained by the OMI for the phytoplankton groups.

Phytoplankton groups	Marginality (OMI)	Tolerance (Tol)	Residual tolerance (*R*Tol)	*p*-value
Cyanobacteria	0.02	2.26	6.52	< 0.01
Coccolithophores	0.59	4.38	5.39	< 0.01
Diatoms	2.35	4.5	5.33	< 0.01
Chlorophytes	3.68	1.98	5.66	< 0.01

For both climatic regimes, the mean environmental condition of the subsets was substantially different from *G*, the general mean conditions ($p < 0.01$). Environmental envelopes were also statistically different, with El Niño displaying a more restricted environmental envelope than La Niña (Figure 4). Higher marginality values corresponded to greater uniqueness of the environmental conditions under which the taxon occurred, and hence, the lower its tolerance compared to *G* or *G_K* (specialist taxa). Furthermore, the higher the tolerance value, the greater the environmental range within which the taxon occurs (generalist taxa), and the higher the residual tolerance value, the weaker the relationship between the taxa distribution and environmental parameters.

The graphical display of the WitOMI analysis within a two-dimensional Euclidean space represents the communities' niche positions in the environmental gradients. WitOMI revealed that increased rainfall, river flux, wind speed, MLD, and NO_3 were associated with La Niña, whereas high values of PAR and SST characterized El Niño conditions. The test for statistical significance (subkrandtest: Monte-Carlo tests) was conducted by comparing the observed community marginality and the simulated values, after 999 random permutations, under the null hypothesis that the taxon is indifferent to its environment (under both El Niño and La Niña conditions). The test was significant for all taxa and the results indicated significant shifts in the sub-niche position of phytoplankton communities under different sets of environmental conditions related to El Niño and La Niña.

The marginality of phytoplankton groups (WitOMI*G_K*) relative to the mean environmental conditions of the subsets (*G_K*) indicated variations in preferences between both ENSO regimes. Cyanobacteria positioned close to *G_K* had the lowest marginality (OMI= 0.02) and displayed the highest residual tolerance implying their occurrence in typical environmental conditions (generalist), and a weak link with the environmental variables encountered. Hence, cyanobacteria used habitats that were the least marginal to El Niño conditions WitOMI*G_K*= 0.02) and La Niña conditions (WitOMI*G_K* = 0.02) with the highest tolerance values

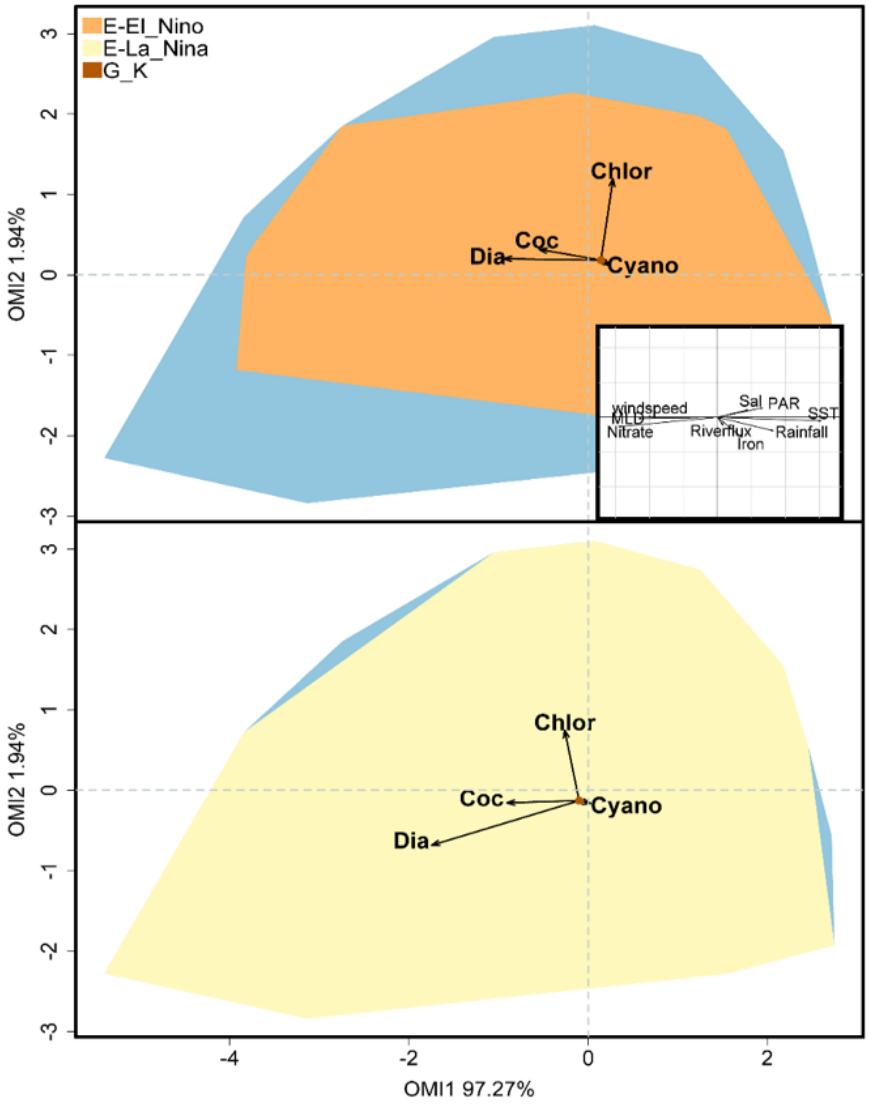

Figure 4. WitOMI analysis comparing the distribution of phytoplankton functional groups between the two climatic regimes (El Niño and La Niña). Orange and yellow polygons represent the subsets for both climatic regimes within the total environment (light blue polygon). For each subset, the centre of gravity of the distribution is indicated (G_K) by a red dot. The origin represents the average environmental conditions G. The axes represent the gradient of hydro-climatic conditions associated with La Niña and El Niño. The length of the arrows corresponds to the marginality of each phytoplankton group within a subset (orange points: SR), relative to G_K, including the canonical weights of environmental variables calculated from the OMI. SST was strongly positively correlated to PCA axis 1 ($r = -0.83$; $p < 0.001$) while salinity PAR and rainfall had a moderate positive correlation with PCA axis 1 ($r = 0.59$, $p = 0.02$). NO_3, wsp and MLD was strongly positively correlated with PCA axis 1 ($r = 0.8$; $p < 0.001$).

Table 4. Marginality (WitOMIG_K) and tolerance (TolG_K) parameters obtained by the WitOMI analysis within each climatic regime.

Climatic regime	Parameter	Cyanobacteria	Coccolithophores	Diatoms	Chlorophytes
El Niño	WitOMIG_K	0.02	0.53	1.29	2.77
	TolG_K	2.49	3.87	3.54	1.33
La Niã	WitOMIG_K	0.02	0.66	3.12	1.76
	TolG_K	2.73	4.91	4.64	1.51

(Tol: 2.49 and 2.73, respectively) (Table 4). Cyanobacteria therefore represented greater independence from environmental conditions during both climatic regimes.

Coccolithophores showed intermediate marginality with high tolerance values (OMI= 0.59; Tol= 4.38). Coccolithophores had the highest tolerance values under both El Niño and La Niña regimes (Tol= 3.87 and 4.91, respectively) but occupied relatively more marginal conditions during El Niño (WitOMIG_K= 0.09) than La Niña (WitOMIG_K= 0.02). Hence a preference for La Niña conditions (Table 4).

Chlorophytes and diatoms with the highest marginalities (OMI= 3.79 and 2.44, respectively) were the most specialist taxa, implying their use of more atypical habitats with a specific range of environmental conditions. Chlorophytes had the highest marginality during El Niño (WitOMIG_K= 2.77) and the lowest tolerance (TolG_K) during both El Niño and La Niña regimes. This means that the environmental conditions encountered during both ENSO regimes strongly limited the abundance and distribution of chlorophytes. In contrast, diatoms occupied environments that were more marginal during La Niña because of higher WitOMIG and WitOMIG_K values (WitOMIG_K= 3.12). All grades within both subsets were significant (999 permutations of the Monte Carlo permutation test; $p < 0.01$) (Table 4).

WitOMI further provided the marginality of phytoplankton communities relative to the environmental envelope (E), corresponding to the range of environmental conditions encountered in the SCS during the study period. The 'niche.parameter' function in the ade4 package calculated the taxa niche (Inertia, OMI, Tol, and RTol) establishing the most crucial environmental drivers of phytoplankton community change, separating the communities based on their niche characteristics. El Niño conditions were associated with high SST, sal, PAR, and high Fe concentrations in surface waters. In contrast, La Niña conditions coincided with stronger winds, deeper mixing, and increased river discharge, contributing to high surface NO_3 concentrations.

3.3 GAM-based non-linear response of phytoplankton communities

To explore the non-linear response of phytoplankton communities over time and during the progression of El Niño / La Niña events, we fitted a GAM to the Niño index. The GAMs models also capture the variability of phytoplankton communities over time and their response to El Niño/La Niña (Table 5). GAM results revealed that the concentration of Chl-*a* and the abundance of coccolithophores did not change significantly over time. Instead, El Niño explained the bulk of the variation in both variables (19% and 18.2%, p-value= 0.000, respectively). In contrast, interannual variability accounted for 14.1% and 20.1% of the variation in cyanobacteria and diatoms, respectively (p-value=9). However, while diatoms increased linearly between 1998 and 2012, cyanobacteria decreased rapidly between 1998 and 2004 and then rose sharply thereafter.

Table 5 shows the combined model fits of the observed versus predicted values of the log-transformed abundances of phytoplankton functional groups and Chl-*a* estimated from GAM-based models. The summary of individual model performance in terms of deviation explained for all model fits and their p-values are provided. These results confirm that coccolithophores and overall primary production are more sensitive to ENSO while cyanobacteria and diatoms are more tolerant to the phenomenon and respond more to other inherent oceanographic parameters linked to the the Asian monsoons.

Table 5. Results of GAM-based smoothed fits of covariates modeling of phytoplankton communities over time and in response to ENSO.

	Niño Index		Time (years)	
Biotic parameters	Variance (%)	p-value < 0.05	Variance (%)	p-value < 0.05
Chl-*a*	19.0	0.000	2.41	0.550
Coc	18.2	0.000	3.81	0.170
Cya	6.63	0.075	14.10	0.000
Dia	13.0	0.005	20.10	0.000

4. Discussion

We analyzed the main drivers of interannual changes in four major phytoplankton communities in the SCS from 1998–2012 and modeled the role of El Niño and La Niña in distinguishing the niche characteristics of individual phytoplankton groups. This study highlights the influence of multiple environmental conditions and ENSO-related climate anomalies on the spatial and temporal variability of phytoplankton functional communities in the SCS. Ndah et al. (2019) previously described multitemporal patterns of phytoplankton dynamics across the entire SCS basin, reporting the increasing trend and northward expansion of cyanobacteria dominance, the declining trend and shrinking spatial extent of coccolithophores, sporadic peaks of diatoms, and the generally low concentrations of chlorophytes between 1998 and 2012.

Overall, SST was the dominant driver of phytoplankton dynamics in the SCS explaining up to 82% of the total variability, and 17% in terms of its pure effect on phytoplankton communities. SST had a particularly strong negative effect on coccolithophores. This explained the spatial dominance of coccolithophores in the relatively cooler NSCS, and the seasonal peak of this community in winter, coinciding with the maximum Chl-*a* concentration (e.g. Ndah et al., 2019). Strong monsoon winds and turbulent mixing intensity during winter (Pan et al., 2015; Huanh et al., 2018; Huynh et al., 2019) coincided with increased coccolithophore concentrations and primary production. In

contrast, cyanobacteria were positively influenced by SST, hence their predominance in the SSCS, a region of relatively high and stable SST. The ability of this group to thrive in warm stratified oligotrophic waters of southern and central SCS (with high summer/autumn abundances) (Ndah et al., 2019) is attributed to their tolerance of high SST and nitrogen-fixing capability, making cyanobacteria e.g., Trichodesmium the main primary producer and the major contributor of N2-fixation in oligotrophic, nitrogen-limited waters (Von Rückert and Giani, 2004) of the SSCS. Therefore, cyanobacteria and probably dinoflagellates were primarily responsible for the weak summer Chl-*a* concentration in the SCS (Ndah et al., 2019). Strong competition from cyanobacteria and other opportunistic taxa such as dinoflagellates may also contribute to the low abundance of chlorophytes.

As an important factor for phytoplankton functional group discrimination across the SCS, Tang and Liu (2020) established that warming winter SSTs during the 1980s and 1990s were responsible for the low primary production. The shared effect of SST and NO_3 explained more than half (51%) of the variability of phytoplankton communities in the SCS. However, only 2% of phytoplankton variability was explained by the pure effect of NO_3, while adding light (PAR) to SST and NO_3 yielded only a weak joint effect of 7%, confirming that individually, the light was a non-limiting factor of phytoplankton variability in the SCS (e.g. Palacz et al., 2011; Liao et al., 2012). Therefore, the monsoon-related influence of SST and a range of mechanisms that modulate the stratification and de-stratification of surface waters also influence nitrogen availability and cumulatively drive the variability of phytoplankton across the SCS. Wu et al. (2003) confirmed that primary production in the oligotrophic SCS surface waters was strongly limited by nitrogen while phosphate (P) concentrations remained relatively high.

Using WitOMI analysis and GAMs, we deduced that ENSO is the primary mechanism that modulates the mix of physicochemical parameters and drives interannual changes in the phytoplankton community structure. El Niño conditions associated with SST spikes induced stratification that reduces vertical mixing and limits NO_3 availability by preventing the upwelling of nutrient-rich waters.

Hence, during the period 2004–2012, the increase in cyanobacteria, the most generalist taxa across the SCS under ENSO conditions, was an indication of El Niño-enhanced warming, vertical stratification, and most likely aolian deposition of Fe. These processes may have contributed to the escalating problem of eutrophication and cyanobacteria blooms in the SCS (e.g. Huppert et al., 2002; Chen et al., 2006; Wang et al., 2010). Chlorophytes, the least abundant group were marginal under both El Niño and La Niña conditions implying that inherent physico-chemical and biological constraints including competition from cyanobacteria were strong limiting factors. van Strien et al. (2012) confirmed that under contemporary environmental conditions, habitat specialists like chlorophytes are typical 'losers' while habitat generalists like cyanobacteria are the 'winners' (the so-called biotic homogenization phenomenon).

One of the primary mechanisms by which El Niño limits nutrient availability is by damping upwelling intensity. Therefore, N-limitation during El Niño was linked to enhanced SST-induced stratification, as high SST $> 30^{\circ}$C is known to drastically reduce nutrient availability limiting primary production (Louanchi and Najjar, 2001). Siswanto et al. (2017) confirmed that upwelling intensity in the SCS declined significantly during the mature phase of El Niño due to weakened Asian winter monsoon winds, and the development of an anticyclonic circulation in the northern and western SCS. These mechanisms are associated with insufficient lifting of the thermocline by wind-driven vertical mixing (Roemmich and McGowan, 1995) and downwelling associated with El Niño-induced anticyclonic circulation limiting new primary production across the SCS. Zhao and Tang (2007), Tan and Shi (2009), and Liao et al. (2012) support the idea of contrasting effects of El Niño on upwelling intensity across different regions in the SCS. Ashok et al. (2007) reported that primary production across the SCS responds differently to two main types of El Niño; a basin-wide decrease in response to canonical El Niño (with a 4-month lag), and an increase in Chl-*a* across central and eastern SCS in response to El Niño Modoki. Tan and Shi (2009) attributed the decline of summer Chl-*a* in western SCS to weakening Ekman pumping/weak upwelling in response to the 1997/1998 El Niño. Overall, a basin-scale decrease in Chl-*a* across the SCS was linked to Ekman downwelling caused by canonical El Niño (Liao et al., 2012) and weakened southwest monsoon winds that generate anticyclonic eddies that intensify the surface stratification, suppressing the upward mixing of nutrients.

Surface Fe enrichment is also associated with El Niño via Southeast Asian dust events and vegetation burning induced by intense drought and forest fires. A previous study by Zhang et al. (2007) confirms that aerosols over the SCS contain up to 16–82% of iron (approx. 0.1 to 0.9 mg m^{-3}). Hence, Fe-enrichment coupled with N-limitation during El Niño may also favor the dominance of cyanobacteria. Therefore, El Niño creates an artificial state of nutrient poverty across the SCS favoring the opportunistic dominance and northward expansion of cyanobacteria at the expense of coccolithophores. In general, El Niño has been associated with very low Chl-*a* over the SCS basin as reported by Palacz et al. (2011) following the 1997/98 El Niño.

In contrast, the first half of our study period (1998 –2004) was dominated by La Niña-like conditions. This is confirmed by studies revealing that most parts of the tropical ocean cooled slightly after the super El Niño of 1997/98 (Ndah, 2017), contributing to an increase in Chl-*a* in the

SCS from 1999 to 2003 following prolonged La Niña conditions (Palacz et al., 2011). Therefore, La Niña-induced cooling drove microbial responses, favoring the increase in coccolithophores, and overall primary production between 1998 and 2004. The decline in cyanobacteria during the same period attests to the competitive dominance of coccolithophores and the negative response of the former taxon to anomalous cooling conditions in the SCS.

The mechanisms by which La Niña drove differences in phytoplankton community structure were associated with the intensification of wind speed, deep vertical mixing of the previously stratified waters injecting cold nitrogen-enriched waters onto the surface, the main limiting nutrient in the SCS, per Wu et al. (2003). La Niña conditions therefore strengthened monsoon winds and intensified turbulent mixing and cyclonic eddies (Pan et al., 2015; Huanh et al., 2018; Huynh et al., 2019; Shih et al., 2020), spurring high coccolithophore concentrations and primary production during the period 1998–2004. Previous studies confirm that intermediate and deep waters from the western Philippine Sea through the Luzon Strait supplied largely by ocean gyres, lateral transport, vertical diapycnal diffusion, eddy mixing dynamics, Kuroshio intrusions, and internal waves are the main source of nutrient input into the photic zone of the SCS (Shih et al., 2020).

The increase in riverine input of sediment-laden waters into the SCS under la Niña conditions (e.g. Cheah et al., 2013; Wang et al., 2013) also acts as an important source of terrigenous nitrogen, increasing phytoplankton biomass. In contrast, the decline in primary production on the west coast of Borneo was attributed to El Niño-related reductions in the riverine supply of nutrients (Sun, 2017) while Siswanto et al. (2017) linked the decline in Chl-*a* off the Vietnamese coast to reduced nutrient loads from the Mekong River at some point of the El Niño gradient, influencing both phytoplankton biomass and general cell size (Groß et al., 2022).

Diatoms appeared as a generalist taxon in nearshore environments with significant tolerance under both El Niño and La Niña conditions. However, the relatively high marginality of this community during La Niña could be partly attributed to low surface Fe concentrations due to reduced atmospheric deposition, despite N availability. Hence, although diatoms account for ~ 20% of global primary production, high concentrations are generally localized in nearshore environments of the SCS likely because they are more limited by the availability of Fe and other trace nutrients such as Cu (Huapaya and Echeveste, 2023) compared to cyanobacteria and coccolithophores. Other studies have shown that diatoms tolerate iron limitation and frequently dominate iron-stimulated phytoplankton blooms (Gao et al., 2021). For this reason, diatom blooms have been frequently reported off the coast of Guangdong (Liu et al., 2011) and in other nearshore environments (e.g., Peng and Wang, 1999; Hodgkiss and Lu, 2004; Gao and Song, 2005; Wang et al. 2006; Wong et al., 2007; Wang et al., 2010) in response to high SST, sal and riverine loadings of dissolved inorganic nitrates and silicates while dinoflagellates dominate occasionally under high phosphate levels (Peng et al., 1999; Wang et al., 2006). We, therefore, surmise that persistent ocean warming and lengthened stratification periods will increase cyanobacteria dominance and its northward expansion in the SCS, in addition to frequent cyanobacteria blooms, and episodic diatom blooms in the nearshore NSCS. In agreement with this assessment, Xu et al., (2019) found that HAB trends in China's Northern Beibu Gulf increased significantly in geographic scale and frequency from six events over a period of 15 years (1985–2000) to 13 over a period of 10-years (2001–2010), and 20 events, in just six years (2011–2017). The authors noted that the cyanobacteria Microcystis aeruginosa, cyanobacteria and dinoflagellates, and Phaeocystis globose, respectively, dominated the three periods (Xu et al., 2019). A subsequent study by Guo et al. (2021) confirmed that, summer algal blooms have grown annually in China's Yellow Sea since 2007, with the 2021 event covering about 1746 km^2, being 2.3 times larger than the previous 2013 record event. The increasing frequency of HAB events in Chinese LMEs including the SCS was linked to the increase in N:P molar ratio above the 25 threshold value from the 1980s in response to the decrease in P and the increased N (Wang et al., 2021). Similarly, Mackey et al. (2017) found that N and Fe enrichment in the adjacent East China Sea were mainly responsible for the frequent summer/spring diatom and dinoflagellate blooms.

5. Conclusions

We have analyzed the effects of concurrent changes in abiotic conditions (SST, light, sal, river flux, MLD, and nutrients) on the variability of diverse phytoplankton communities in the SCS at the 'large marine ecosystem' scale, during the period 1998–2012. This study extends knowledge of microbial communities' response to ENSO-related climatic anomalies by providing evidence of the multifaceted responses of hydrographic conditions and phytoplankton communities in relation to El Niño and La Niña. Our results supplement previous studies conducted largely in nearshore coastal locations and at intra-annual time scales. We conclude that El Niño Southern Oscillation (ENSO) is the dominant driver of inter-annual variability shaping phytoplankton community structure. These environmental conditions influenced niche occupation and constrained changes in phytoplankton communities by influencing nutrient availability and variability in space and time. Therefore, El Niño-related stratification influences phytoplankton dynamics by limiting NO_3 concentration in the photic zone limiting primary production despite the iron-enrich state of the SCS. We posit that El Niño creates an artificial state of nutrient poverty across the SCS by limiting the input and re-suspension of nutrients (primarily NO_3) nec-

essary for primary production, favoring the opportunistic dominance and the northward expansion of cyanobacteria across the SCS basin while limiting coccolithophores abundance due to their natural preference for cold nitrate rich-waters in north-eastern SCS. Diatom blooms rely on the window of opportunity created when ENSO-related hydrographic conditions entrain diatom cells in the photic zone, coinciding with high NO_3 concentrations and Fe-enriched surface waters. Our results demonstrate that ENSO was mostly responsible for inter-annual SST changes and phytoplankton dynamics in the SCS during the study period. El Niño-induced warming dampened monsoon wind intensity, limiting vertical mixing and simultaneously decreasing rainfall and river discharge. These mechanisms influenced changes in iron and nitrate concentrations in space and time driving changes in phytoplankton communities and their spatial patterns. These results are relevant in the context of ongoing anthropogenic and climatic changes driving ecosystems towards warmer stratified conditions resulting in decreased primary production and declining coccolithophores, with implications for the carbon cycle and carbonate system. These results highlight the need to incorporate El Niño-induced atmosphere-ocean interactions into future studies and models to assess the effects of climatic change on marine biogeochemistry and plankton dynamics. We also demonstrate the importance of time series datasets and mixed multivariate approaches to investigate complex non-linear interactions. We recognize the need for future modeling studies to fully appraise the impacts of climatic and anthropogenic changes on phytoplankton communities at much longer time scales focusing simultaneously on the Northern and Southern SCS. These findings highlight the need to incorporate interannual climatic oscillations into models assessing multiple stressor effects on marine ecology in the tropical/subtropical ocean and could guide efforts toward sustainable ocean management in the context of climate change.

Declaration of competing interest

The authors declare that they have no known competing financial interests or personal relationships that could have appeared to influence the work reported in this paper.

References

Ashok, K., Behera, S.K., Rao, S.A., Weng, H., Yamagata, T., 2007. *El Niño Modoki and its possible teleconnection*. J. Geophys. Res. 112, C11007. https://doi.org/10.1029/2006JC003798

Alves-de-Souza, C., Iriarte, J.L., Mardones, J.I., 2019. *Interannual Variability of Dinophysis acuminata and Protoceratium reticulatum in a Chilean Fjord: Insights from the Realized Niche Analysis*. Toxins 11(1), 19. https://doi.org/10.3390/toxins11010019

Baker, M.E., King, R.S., 2010. *A new method for detecting and interpreting biodiversity and ecological community thresholds*. Methods Ecol. Evol. 1, 25–37. https://doi.org/10.1111/j.2041-210X.2009.00007.x

Bajarias, F.F.A., 2000. *Phytoplankton in the surface layers of the South China Sea, Area III: Western Philippines*. [in:] Proceedings of the Third Technical Seminar on Marine Fishery Resources Survey in the South China Sea, Area III: Western Philippines, 13–15 July 1999. Bangkok, Thailand, Secretariat, Southeast Asian Fisheries Development Center, 220–234. Retrieved January, 2016, from: http://repository.seafdec.org/handle/20.500.12066/4355

Birk, S., Chapman, D., Carvalho, L. et al., 2020. *Impacts of multiple stressors on freshwater biota across spatial scales and ecosystems*. Nat. Ecol. Evol. https://doi.org/10.1038/s41559-020-1216-4

Borcard, D., Gillet, F. , Legendre, P., 2011. *Numerical Ecology with R.*, 1st edn., Springer Int. Publ. AG, Switzerland, 436 pp., ISBN: 978-1-4419-7975-9. https://doi.org/10.1007/978-1-4419-7976-6

Cheah, W., Taylor, B.B., Wiegmann, S., Raimund, S., Krahmann, G., Quack, B., Bracher, A., 2013. *Photophysiological state of natural phytoplankton communities in the South China Sea the Sulu Sea*. Biogeosci. Discuss. 10. http://dx.doi.org/10.5194/bgd-10-12115-201

Chen, C.C., Shiah, F.K., Chung, S.W., Liu, K.K., 2006. *Winter phytoplankton blooms in the shallow mixed layer of the South China Sea enhanced by upwelling*. J. Marine Syst. 59, 97–110. https://doi.org/10.1016/j.jmarsys.2005.09.002

Cota, S.S., Borrego, S.A., 1988. *The El Niño effect on the phytoplankton of a northwestern Baja California coastal lagoon*. Estuar. Coast. Shelf Sci. 27(1), 109–115. https://doi.org/10.1016/0272-7714(88)90034-0

Cui, D., Wang, J., Tan, L., 2016. *Response of phytoplankton community structure and size-fractionated chlorophyll-a in an upwelling simulation experiment in the Western South China Sea*. J. Ocean Univ. China Oceanic & Coastal Sea Res. 15(5), 835–840. https://doi.org/10.1007/s11802-016-3017-6

DeVantier, L.M., Turak, E., 2009. *Coral Reefs of Brunei Darussalam*. Fisheries Dept., MIPR, Brunei Darussalam, 100 pp., ISBN: 978-99917-31-48-3.

Dolédec, S., Chessel, D., Gimaret-Carpentier C., 2000. *Niche Separation in Community Analysis: a New Method*. Ecology 81, 2914. https://doi.org/10.1890/0012-9658(2000)081[2914:NSICAA]2.0.CO;2

Dong, L., Li, L., Li, Q., Liu, J., 2015. *Basin-wide distribution of phytoplankton lipids in the South China Sea during intermonsoon seasons: influence by nutrient and physical dynamics*. Deep Sea Res. Pt. II 122, 52–63. https://doi.org/10.1016/j.dsr2.2015.07.005

Gao, X.L., Song, J.M., 2005. *Phytoplankton distributions and their relationship with the environment in the Changjiang. Estuary, China*. Mar. Pollut. Bull. 50 (3), 327–335. https://doi.org/10.1016/j.marpolbul.2004.11.004

Gao, X.L., Bowler, C., Kazamia, E., 2021. *Iron metabolism strategies in diatoms*. J. Experiment. Botany 72(6), 2165–2180. https://doi.org/10.1093/jxb/eraa575

Giehl, N.F.S., Brasil, L.S., Dias-Silva, K., Nogueira, D.S., Cabette, H.S.R., 2019. *Environmental Thresholds of Nepomorpha in Cerrado Streams, Brazilian Savannah*. Neotrop. Entomol. 482, 186–196. https://doi.org/10.1007/s13744-018-0632-5

Gieswein, A., Hering, D., Lorenz, A.W., 2019. *Development and validation of a macroinvertebrate-based biomonitoring tool to assess fine sediment impact in small mountain streams*. Sci. Total Environ. 652, 1290–1301. https://doi.org/10.1016/j.scitotenv.2018.10.180

Groß, E., Di Pane, J., Boersma, M., Meunier, C.L., 2022. *River discharge-related nutrient effects on North Sea coastal and offshore phytoplankton communities*. J. Plankton Res. 44(6), 947–960.

Guisan, A., Edwards, Jr. T.C., Hastie, T., 2002. *Generalized linear and generalized additive models in studies of species distributions: setting the scene*. Ecol. Modell. 157(2–3), 89–100. https://doi.org/10.1016/S0304-3800(02)00204-1

Guo, C., Yu, J., Ho, T.-Y., Wang, L., Song, S., Kong, L., Liu, H., 2012. *Dynamics of phytoplankton community structure in the South China Sea in response to the East Asian aerosol input*. Biogeosciences 9, 1519–1536. https://doi.org/10.5194/bg-9-1519-2012

Guo, X., Yu, Y., Zhu, H., Zhao, X., Liu, X., 2020. *Multivariate analysis of phytoplankton community structure in Changli Gold Coast National Nature Reserve of Hebei Province in spring, 2019*. IOP Conf. Ser.: Earth Environ. Sci. 467, 012141. https://doi.org/10.1088/1755-1315/467/1/012141

Guo, X., Zhu, A., Chen, R., 2021. *China's algal bloom suffocates marine life*. Science. 373 (6556), 751. https://doi.org/10.1126/science.abl5774

Hodgkiss, I.J., Lu, S.H., 2004. *The effects of nutrients and their ratios on phytoplankton abundance in Junk Bay, Hong Kong*. Hydrobiol. 512, 215–229. https://doi.org/10.1023/B:HYDR.0000020330.37366.e5

Huang, K.-F., You, C.-F., 2007. *Tracing freshwater plume migration in the estuary after a typhoon event using Sr isotopic ratios*. Geophys. Res. Lett. 34, L02403. https://doi.org/10.1029/2006GL028253

Huapaya, K., Echeveste, P., 2023. *Physiological responses of Humboldt current system diatoms to Fe and Cu colimitation*. Mar. Environ. Res. 187(30), 105937. https://doi.org/10.1016/j.marenvres.2023.105937

Huppert, A., Blasius, B., Stone, L., 2002. *A model of phytoplankton blooms*. Am. Nat. 159(2) 156–171. https://doi.org/10.1086/324789

Huynh, H-N.T. Alvera-Azcárate, A., Beckers, J-M., 2019. *Analysis of surface Chl-a associated with sea surface temperature and surface wind in the South China Sea*. Ocean Dynam. 705. https://doi.org/10.1007/s10236-019-01308-9

Hsu, S.-C., Gong, G.-C., Shia, F.-K. et al., 2014. *Sources, solubility, and acid processing of aerosol iron and phosphorous over the South China Sea: East Asian dust and pollution outflows vs. Southeast Asian biomass burning*. Atmos. Chem. Phys. Discuss. 14, 21433–21472. https://doi.org/10.5194/acpd-14-21433-2014

IHO, 1953. *Limits of Oceans and Seas*. International Hydrographic Organization. Bremerhaven, PANGAEA, hdl:10013/epic.37175.d001, https://epic.awi.de/id/eprint/29772/1/IHO1953a.pdf

Karasiewicz, S., Dolédec, S., Lefebvre, S., 2017. *Within outlying mean indexes: refining the OMI analysis for the realized niche decomposition*. PeerJ 5:e3364. https://doi.org/10.7717/peerj.3364

King, R.S., Baker, M.E., Kazyak, P.F., Weller, D.E., 2011. *How novel is too novel? Stream community thresholds at exceptionally low levels of catchment urbanization*. Ecol. Appl. 215, 1659–78. https://doi.org/10.1890/10-1357.1

Legendre, P., Legendre., L., 2012. *Numerical ecology*. 3rd edn., Elsevier Sci. BV, Amsterdam. xvi + 990 pp.

Li, Q.P., Dong, Y., Wang, Y., 2015a. *Phytoplankton dynamics driven by vertical nutrient fluxes during the spring intermonsoon period in the north-eastern South China Sea*. Biogeosci. Discuss. 12, 6723–6755. https://doi.org/10.5194/bgd-12-6723-2015

Li, Q.P., Wang, Y.J. Dong, Y. Gan, J.P. et al., 2015b. *Modeling long-term change of planktonic ecosystems in the northern South China Sea and the upstream Kuroshio Current*. J. Geophys. Res. 120(6), 3913–3936. https://doi.org/10.1002/2014JC010609

Liao, X., Ma, J., Zhan, H., 2012. *Effect of different types of El Niño on primary productivity in the South China Sea*. Aquat. Ecosyst. Health 15, 135–143. https://doi.org/10.1080/14634988.2012.687655

Lin, I.-I., Lien, C.-C., Wu, C.-R., Wong, G.T.F., Huang, C.-W., Chiang, T.-L., 2010. *Enhanced primary production in the oligotrophic South China Sea by eddy injection in spring*. Geophys. Res. Lett. 37, L16602. https://doi.org/10.1029/2010GL043872

Liu, H., Song, X., Huang, L., Tan, Y., Zhang, J., 2011. *Phytoplankton biomass and production in the northern South China Sea during summer: Influenced by Pearl River discharge and coastal upwelling*. Acta Ecol. Sin. 31, 133–136. https://doi.org/10.1016/J.CHNAES.2011.02.001

Louanchi, F., Najjar, R.G., 2001. *Annual cycles of nutrients and oxygen in the upper layers of the North Atlantic Ocean*. Deep Sea Res. Pt. II: Top. Stud. Oceanogr. 4810, 2155–2171. https://doi.org/10.1016/S0967-06450000185-5

Lu, S.H., Hodgkiss, I.J., 1999. *An unusual year for the occurrence of harmful algae*. Harmful Algal News 18, 1–3.

Lu, S., Hodgkiss, I.J., 2004. *Harmful algal bloom causative collected from Hong Kong waters*. [in:] Ang P.O., (ed.), *Asian Pacific Phycology in the 21st Century: Prospects and Challenges. Developments in Hydrobiology*. Springer, Dordrecht, 173 pp. https://doi.org/10.1007/978-94-007-0944-7_30

Mackey, K.R.M., Kavanaugh, M.T., Wang, F. et al., 2017. *Atmospheric and Fluvial Nutrients Fuel Algal Blooms in the East China Sea*. Front. Mar. Sci. 4. https://doi.org/10.3389/fmars.2017.00002

Meehl, G.A., Arblaster, J.M., Fasullo, J.T., Hu, A., Trenberth, K.E., 2011. *Model-based evidence of deep-ocean heat uptake during surface-temperature hiatus periods*. Nat. Clim. Change 1(7), 360–364. http://dx.doi.org/10.1038/nclimate1229

Meehl, G.A., Teng, H., Arblaster, J.M., 2014. *Climate model simulations of the observed early-2000s hiatus of global warming*. Nat. Clim. Change 4(10), 898–902. https://www.nature.com/articles/nclimate2357

Milliman, J.D., Mie-e, R., 1995. *River flux to the sea: impact of human intervention on river systems and adjacent coastal areas*, [Chapter 4]. [in:] Eisma, D., (ed.), *Climate Change: Impact on coastal habitation*, Lewis Publ., Boca Raton, 57–84.

Moreno, H.D., Köring, M., Di Pane, J. et al., 2022. *An integrated multiple driver mesocosm experiment reveals the effect of global change on planktonic food web structure*. Commun Biol. 5, 179 pp. https://doi.org/10.1038/s42003-022-03105-5

NCDC, 2003. *El Niño/Southern Oscillation – Annual 2004*. NOAA National Centres for Environmental Information. Retrieved October, 2020, from: https://www.ncdc.noaa.gov/sotc/enso/200313

NCDC, 2004. *El Niño/Southern Oscillation – Annual 2004*. NOAA National Centres for Environmental Information. Retrieved October, 2020, from: https://www.ncdc.noaa.gov/sotc/enso/200413

NCDC, 2009. *El Niño/Southern Oscillation – September 2009*. NOAA National Centres for Environmental Information. Retrieved February, 2020, from: https://www.ncdc.noaa.gov/sotc/enso/200909

Ndah, A.B., 2017. *Multi-temporal patterns of sea surface temperature in the South China Sea: a perfect reflection of global ocean-climatic variability modes?*, 18th Int. GHRSST Sci. Team Meeting, Qingdao, China, 5–9 June 2017. Retrieved March, 2019, from: https://www.researchgate.net/publication/320161672_multi-temporal_patterns_of_sea_surface_temperature_in_the_south_china_sea_a_perfect_reflection_of_global_ocean-climatic_variability_modes

Ndah, A.B., Dagar, L.K., Becek, B., Odihi, J.O., 2019. *Spatio-temporal dynamics of phytoplankton functional groups in the South China Sea and their relative contributions to marine primary production*. Region. Stud. Mar. Sci. 29, 100598. https://doi.org/10.1016/j.rsma.2019.100598

Ning, X., Chai, F., Xue, H., Cai, Y., Liu, C., Shi, J., 2004. *Physical-biological oceanographic coupling influencing phytoplankton and primary production in the South China Sea*. J. Geophys. Res. 109, C10005. https://doi.org/10.1029/2004JC002365

Palacz, A. P., Xue, H., Armbrecht, C., Zhang, C., Chai, F., 2011. *Seasonal and inter-annual changes in the surface chlorophyll of the South China Sea*. J. Geophys. Res. 116, C09015. https://doi.org/10.1029/2011JC007064

Pedersen, E.J, Miller, D.L., Simpson, G.L., Ross, N., 2019. *Hierarchical generalized additive models in ecology: an introduction with mgcv*. PeerJ 7:e6876. https://doi.org/10.7717/peerj.6876

Peng, Y., Wang, Z., 1999. *Analysis of nutritive status and variation of hydrochemical indexes in seawater of aquaculture area at Dapeng'ao Bight in Daya Bay*. J. Oceanogr. Taiwan Strait 18(1), 26–32.

Phang, S-M., Yeong, Y.H., Ganzon-Fortes, E.T. et al., 2016. *Marine algae of the South China Sea is bordered by Indonesia, Malaysia, Philippines, Singapore, Thailand and Vietnam*. Raffles Bull. Zool. 34, 13–59. https://doi.org/10.1007/A43C-165932685F02

Qiu, D.J., Huang, L.M., Zhang, J.L., Lin, S.J., 2010. *Phytoplankton dynamics in and near the highly eutrophic Pearl River Estuary, South China Sea*. Continent. Shelf Res. 30(2), 177–186. https://doi.org/10.1016/j.csr.2009.10.015

Raitsos, D.E., Lavender, S.J., Maravelias, C.D., Haralabous, J., Richardson, A.J., Reid, P.C., 2008. *Identifying four phytoplankton functional types from space: An ecological approach*. Limnol. Oceanogr. 532, 605–613. https://doi.org/10.4319/lo.2008.53.2.0605

Roemmich, D., McGowan, J., 1995. *Climatic warming and the decline of zooplankton in the California Current*. Science 267, 5202, 1324–1326. https://doi.org/10.1126/science.267.5202.1324

Shen, P.-P., Li, G., Huang, L.-M., Zhang, J.-L., Tan, Y.-H., 2011. *Spatio-temporal variability of phytoplankton assemblages in the Pearl River estuary, with special reference to the influence of turbidity and temperature*. Cont. Shelf Res. 31(16), 1672–1681. https://doi.org/10.1016/j.csr.2011.07.002

Shih, Y-Y., Hung, C-C., Tuo, S., et al., 2020. *The Impact of Eddies on Nutrient Supply, Diatom Biomass and Carbon Export in the Northern South China Sea*. Front. Earth Sci. 8, 537332.

https://doi.org/10.3389/feart.2020.537332

Simpson, G.L., 2018. *Modelling Palaeoecological Time Series Using Generalized Additive Models*. Front. Ecol. Evol. 6, 149. https://doi.org/10.3389/fevo.2018.00149

Siswanto, E., Ye, H., Yamazaki, D. and Tang, D.L., 2017. *Detailed spatiotemporal impacts of El Niño on phytoplankton biomass in the South China Sea*. J. Geophys. Res. Oceans 122, 2709–2723. https://doi.org/10.1002/2016JC012276

Sultana, J., Tibby, J., Recknagel, F., Maxwell, S., Goonan, P., 2020. *Comparison of two commonly used methods for identifying water quality thresholds in freshwater ecosystems using field and synthetic data*. Sci. Total Environ. 724, 137999. https://doi.org/10.1016/j.scitotenv.2020.137999

Sun, C., 2017. *Riverine inluence on ocean color in the equatorial South China Sea*. Cont. Shelf Res. 143, 151–158. https://doi.org/10.1016/j.csr.2016.10.008

Tan, S.C., Shi, G.Y., 2009. *Spatiotemporal variability of satellite-derived primary production in the South China Sea, 1998–2006*. J. Geophys. Res. 114, G03015. https://doi.org/10.1029/2008JG000854

Tan, S., Zhang, J., Li, H. et al., 2020. *Deep Ocean Particle Flux in the Northern South China Sea: Variability on Intra-Seasonal to Seasonal Timescales*. Front. Earth Sci. 8, 74. https://doi.org/10.3389/feart.2020.00074

Tang, D.L., Ni, I.H., Kestner, D.R., Muller-Kargen, F.E., 1999. *Remote sensing observations of winter phytoplankton blooms southeast of the Luzon Strait in the South China Sea*. Mar. Ecol. Prog. Ser. 191, 43–51. https://doi.org/10.3354/meps191043

Tang, D.L., Kawamura, H., Dien, T.V., Lee, M.A., 2004. *Offshore phytoplankton biomass increase and its oceanographic causes in the South China Sea*. Mar. Ecol. Prog. Ser. 268, 31–41. https://doi.org/10.3354/meps268031

Tang, S. and Liu, F., 2020. *Remote sensing of phytoplankton declined during the late 1980s and early 1990s in the South China Sea*. Int. J. Remote Sens. 41, 6010–6021. https://doi.org/10.1080/01431161.2020.1718241

Tian, Y.Q., Huang, B., Yu, C., Chen, N.W., Hong, H.S., 2014. *Dynamics of phytoplankton communities in Jiangdong Reservoir, Jiulong River, Fujian, China. Chin*. J. Oceanol. Limnol. 32(2) 255–265. https://doi.org/10.1007/s00343-014-3158-7

Trenberth, K., Nat. Center Atmospheric Res.Staff (Eds.), 2020. *The Climate Data Guide: Niño SST Indices Niño 1+2, 3, 3.4, 4; ONI and TNI*. Retrieved November, 2019, from: https://climatedataguide.ucar.edu/climate-data/Ni~{n}o-sst-indices-Ni~{n}o-12-3-34-4-oni-and-tni

Turak, E., DeVantier, L.M., 2011. *Field Guide to Reef-building Corals of Brunei Darussalam*. Fisheries Dept., MIPR, Brunei Darussalam, 256 pp., ISBN: 978-99917-31-49-0.

van Strien, A.J., Soldaat, L.L., Gregory, R.D., 2012. *Desirable mathematical properties of indicators for biodiversity change*. Ecol. Indic. 14, 202–208. https://doi:10.1016/j.ecolind.2011.07.007

Von Rückert, G., Giani, A., 2004. *Effect of nitrate and ammonium on the growth and protein concentration of Microcystis viridis Lemmermann cyanobacteria*. Rev. Bras. Bot. 27(2). https://doi.org/10.1590/S0100-84042004000200011

Wang, Z.-D., Ho, K.-C., 2002. *Oceanographic conditions of the South China Sea continental shelf*. Retrieved January, 2015, from: http://www.red-tide.org/new_site/ocean_con.htm

Wang, Z., Qi, Y. Chen, J., Xu, N., Yang Y., 2006. *Phytoplankton abundance, community structure, and nutrients in cultural areas of Daya Bay, South China Sea*. J. Mar. Syst. 62, 85–94. https://doi.org/10.1016/j.jmarsys.2006.04.008

Wang, J.J., Tang, D.L., Sui, Y., 2010. *Winter phytoplankton bloom induced by subsurface upwelling and mixed layer entrainment southwest of Luzon Strait*, J. Mar. Syst. 83, 141–149.

Wang, G., Cao, W., Wang, G., Zhou, W., 2013. *Phytoplankton size class derived from phytoplankton absorption and chlorophyll-a concentrations in the northern South China Sea*. Chinese J. Oceanol. Limnol. 31(4), 750–761. http://dx.doi.org/10.1007/s00343-013-2291-z

Wang, Y., Zhao, M., Dai, C., Pan, X., 2014. *Nonlinear dynamics of a nutrient-plankton model*. Abstract Appl. Analysis, Hindawi Publ. Corp., 451757, 10. http://dx.doi.org/10.1155/2014/451757

Wang, J., Bouwman, A.F., Liu, X. et al., 2021. *Harmful algal blooms in Chinese coastal waters will persistdue to pertur bed nutrientratios*. Environ. Sci. Technol. Lett. 8(3), 276–284.

Wei, N., Thangaraj, Ian, S., Jenkinson, R. et al., 2018. *Factors driving the spatiotemporal variability in phytoplankton in the Northern South China Sea*. Cont. Shelf Res. 162. https://doi.org/10.1016/j.csr.2018.04.009

Wong, G.T.F., Tseng, C.M., Wen, L.S., Chung, S.W., 2007. *Nutrient dynamics and N-anomaly at the SEATS station*. Deep Sea Res. Pt. II 54(14), 1528–1545. http://dx.doi.org/10.4319/lo.2008.53.5_part_2.2226

Wood, S.N., 2004. *Stable and efficient multiple smoothing parameter estimation for generalized additive models*. J. Am. Sta. Assoc. 99, 673–686. https://doi.org/10.2307/27590439

Wu, J., Chung, S.-W., Wen, L.-S., Liu, K.-K., Chen, Y.-L.L. Chen, H.-Y., Karl, D.M., 2003. *Dissolved inorganic phosphorus, dissolved iron, and Trichodesmium in the oligotrophic South China Sea*. Global Biogeochem. Cy. 171, 1008. https://doi.org/10.1029/2002GB001924

Xu, Y., Zhang. T., Zhou, J., 2019. *Historical Occurrence of Algal Blooms in the Northern Beibu Gulf of China and Implications for Future Trends*. Front. Microbiol. 10, 451, PMID: 30918499; PMCID: PMC6424905. https://doi.org/10.3389/fmicb.2019.00451

Zhao, H., Tang, D., 2007. *Effect of 1998 El Niño on the distribution of phytoplankton in the South China Sea*. J. Geophys. Res. 112, C02017. https://doi.org/10.1029/2006JC003536

Zhang, X., Zhuang, G., Guo, J., Yin, K. Zhang, P., 2007. *Characterization of aerosol over the Northern South China Sea during two cruises in 2003*. Atmos. Environ. 41, 7821–783. https://doi.org/10.1016/j.atmosenv.2007.06.031